Solar Energy Materials and Solar Cells 191 (2019) 350–355

Contents lists available at ScienceDirect

Solar Energy Materials and Solar Cells

journal homepage: www.elsevier.com/locate/solmat

Light-soaking enhanced passivation of Al_2O_3 on crystalline silicon surface

Meng Xie, Xuegong Yu*, Xiaodong Qiu, Deren Yang*

State Key Laboratory of Silicon Materials and School of Materials Science and Engineering, Zhejiang University, Hangzhou 310027, People's Republic of China

ARTICLE INFO

Keywords:
Silicon
Ultrathin Al_2O_3
Surface passivation
Light-induced enhancement
Trap site

ABSTRACT

Negatively charged ultrathin Al_2O_3 film deposited by atomic layer deposition (ALD) technique has been widely applied in photovoltaic industry because of its excellent passivation effect on both *p* and *n* type silicon surfaces. In this study, we have observed an enhancement of the Al_2O_3 passivation on the surface of *p* type gallium doped Czochralski silicon under illumination, with a rapid effective lifetime increase by ~90%. However, such passivation effect is not stable in dark circumstance at room temperature, with a slow effective lifetime degradation to the initial value. Furthermore, we have confirmed that the enhancement process under illumination and the degradation process in dark are both thermally activated with activation energies of 0.31 ± 0.02 eV and 0.50 ± 0.07 eV, respectively. The capacitance-voltage (C-V) measurements based on the Al/Al_2O_3/*p*-Si capacitor demonstrate that the negative charge at the interface between ultrathin Al_2O_3 film and *p*-Si substrate increases from 7.4×10^{11} cm^{-2} to 9.1×10^{12} cm^{-2} after 1 h's illumination and then returns to the initial value in dark at room temperature after 3 h. This light induced enhancement effect is wavelength dependent and the cut-off wavelength is in the range of 780–800 nm. Based on these results, we have proposed a model to explain the light-soaking enhanced passivation of Al_2O_3 on crystalline silicon surface based on a charge trapping and detrapping process.

1. Introduction

With the prevalence of advanced solar cells like passivated emitter and rear contact (PERC) solar cells, ultrathin atomic layer deposition (ALD) Al_2O_3 (< 10 nm) films passivation have become a more and more significant surface passivation technology, which has attracted intensive interest recently. Ultrathin Al_2O_3 films has been applied and provided excellent surface passivation on the rear side of PERC solar cells [1–3], without inducing the so-called 'parasitic shunting' [3,4]. This phenomenon can be attributed to the high density of negative fixed charge in a range of 10^{12}–10^{13} cm^{-2} near the Al_2O_3/Si interface and the low interface state density of 10^{11} $cm^{-2}.eV^{-1}$ [5–8], depending on the growth conditions. However, it should be noted that the initial deposited Al_2O_3 films usually have weak passivation effects, and a post annealing process is indispensable to activate the excellent passivation [5,9,10]. During the post annealing process, an ultrathin silicon oxide (SiO_x) layer will grow at the Al_2O_3/Si interface, which can reduce the interface state density, and therefore the reconstruction of the Al_2O_3 at the SiO_x/Al_2O_3 interface will lead to an increase of the negative charge near the interface [7,11,12]. However, the passivation of ultrathin Al_2O_3 films has been reported to drastically degrade during the firing process of metal contact formation for the standard solar cells manufacture (~ 800 °C) [13,14], partly due to the blistering of Al_2O_3 [15–17]. The deposition of SiN_x layers by PECVD on the ultrathin Al_2O_3 films could improve the high temperature stability [9,13,14,18]. Meanwhile, an annealing at about 400 °C after the firing process was also proven to significantly improve the degraded effective lifetime [19,20]. Even though the passivation of Al_2O_3 on silicon surface has been intensively investigated, most of the studies are performed in dark circumstances. More interestingly, the enhancement of the passivation of ultrathin Al_2O_3 under illumination has been reported by a few publications [20–23]. However, the mechanism on the enhancement of the ultrathin Al_2O_3 passivation is not clear yet, and further investigation is necessary to understand the passivation mechanism of ultrathin Al_2O_3 under illumination.

In this contribution, we focus on the mechanisms of Al_2O_3 passivation on silicon surface under illumination and the subsequent degradation process. The kinetic processes of the enhancement and subsequent degradation have been systematically studied. Meanwhile, capacitance-voltage (C-V) measurements based on the Al/Al_2O_3/*p*-Si capacitor were carried out to inspect the variation of the charges at the interface of Al_2O_3/*p*-Si. Moreover, the dependence of the enhancement effects on the wavelength has been studied. Furthermore, we have proposed a trapping and detrapping model. These results are of great

* Corresponding author.
E-mail addresses: yuxuegong@zju.edu.cn (X. Yu), mseyang@zju.edu.cn (D. Yang).

https://doi.org/10.1016/j.solmat.2018.11.034
Received 14 February 2018; Received in revised form 23 November 2018; Accepted 26 November 2018
Available online 11 December 2018
0927-0248/

significance for us to understand the light-induced enhancement of Al_2O_3 passivation on the photovoltaic silicon surface.

2. Experiments details

The experimental samples originate from *p*-type gallium-doped < 100 > oriented 15.6 × 15.6 cm^2 Czochralski (CZ) silicon wafers (200 ± 10 μm, 1–3 Ω cm). Before the deposition of ALD-Al_2O_3 films, the wafers underwent an acidic etching to remove the damage layer on Si wafers and a standard Radio Corporation of America (RCA) cleaning. The thermal ALD deposition was carried out on both sides of the wafers at 250 °C, and the trimethylaluminium (TMA) [$Al(CH_3)_3$] were chosen as the gas sources. 70 ALD cycles resulted in 7 nm ultrathin Al_2O_3 films with a deposition rate of 4 s per cycle.

Subsequently, the 15.6 × 15.6 cm^2 sized wafers were cut into 4 × 4 cm^2 small samples, and underwent a post annealing process at 425 °C in N_2 ambient for 30 min to activate the excellent passivation. Then, a rapid thermal process (RTP) at 800 °C for 15 s was applied to simulate the firing contact process in the standard solar cells manufacture. The wafers were illuminated at different temperatures under the full-wave ranged halogen lamp with a power intensity of 30 mW cm^{-2}. After the illumination, the samples were kept in dark at different temperatures. In addition, various long pass optical filters (LPOF) that could only transmit the light above the cut-off wavelength was used to study the influence of the photon energy on the light-soaking enhanced passivation process.

The effective lifetime of each sample was determined by the microwave photoconductance decay technique (MWPCD, WCT-2000, Semilab) at room temperature (23 ± 2 °C). Note that the samples have to be removed from the illumination system for the lifetime measurement. For C-V measurements, the Al/Al_2O_3/*p*-Si MIS capacitor was used, where the 50 nm Al gate electrode was deposited by a thermal evaporation method and the InGa eutectic solution was rubbed on the backside. The measurement was based on the deep-level transient spectroscopy (DLTS) C-V system with a frequency of 1 MHz.

3. Results and discussions

Fig. 1 demonstrates the variation of effective lifetime with the illumination time under the illumination intensity of 30 mW cm^{-2} at 60 °C and the time dependence of the effective lifetime in dark at 23 °C after the illumination. It should be noted that the samples here are the ones that underwent the RTP process after the 425 °C annealing process if not stated specifically. It has been demonstrated in Fig. 1 that the

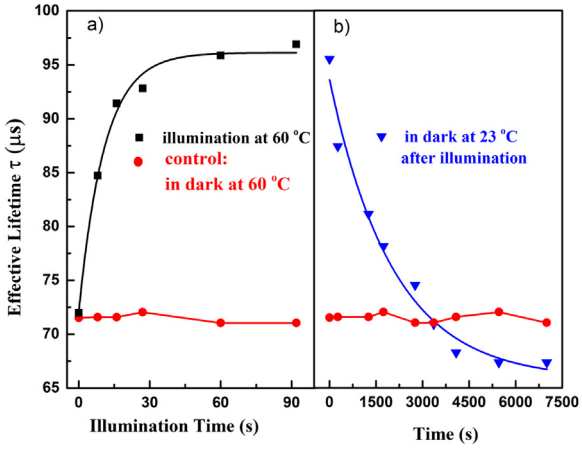

Fig. 1. The effective lifetime as a function of illumination time under illumination with the intensity of 30 mW cm^{-2} at 60 °C (a) and as a function of time in dark at 23 °C (b). The sample kept in dark at 60 °C is chosen as the reference and the curves are guided for eyes.

effective lifetime of the sample illuminated at 60 °C increases by 34% from the initial value of 71.9 μs to the saturated value of 96.9 μs steeply in less than 90 s. Nevertheless, the increased effective lifetime degrades slowly almost to the initial value when the illuminated sample is subsequently stored in dark at room temperature of about 23 °C. However, we can see that the effective lifetime of the controlled sample that is only stored in dark at 60 °C keeps unchanged, which identifies that the increased lifetime is not attributed to the thermal annealing at 60 °C. It can be seen that the saturated effective lifetime is a little smaller than the initial value before illumination, which may be attributed to the damage of the ultrathin Al_2O_3 films during the multiple measurements of effective lifetime. It is obvious that the degradation rate of the effective lifetime in dark is much smaller than the enhancement rate under illumination. In addition, it must be mentioned that the enhancement rate under illumination of the effective lifetime in our work is much larger than that reported in the contribution of Liao et al. [22]. The differences can be explained by the fact that the illumination temperature in our experiments is higher (60 °C) than that in their work (25 °C), and the differences may be also caused by the different sample preparation processes, where our sample underwent additional RTP process after the activation annealing process compared to their sample.

We have carried out the experiments at different temperatures under the illumination intensity of 30 mW cm^{-2} to study the influence of temperatures on the enhancement process, which are demonstrated in Fig. 2. Fig. 2(a) depicts the illumination dependence of the effective lifetime at different temperatures and the inset is the sharp increase of the effective lifetime in the first 40 s Fig. 2(b) demonstrates the Arrhenius plot of the enhancement rate ln(R_{ge}) as a function of the reciprocal of temperatures. The enhancement rate R_{ge} can be given by the following double exponential:

$$\tau(t) = A_1 + k_{11}\exp(R_{ge1}t) + k_{12}\exp(R_{ge2}t) \quad (1)$$

where $\tau(t)$, A_1, k_{11} and k_{12} are the effective lifetime at illumination time t and the calculation constants, respectively. It should be noted that the lifetime enhancement process has been reported to be composed of a fast process and a slow process [22]. In our manuscript, R_{ge1} and R_{ge2} represent the fast and the slow enhancement rates, respectively and the extracted activation energy is the activation energy of the slow process. As shown in Fig. 2(a), the curves determined by the formula (1) fit the measured data very well, which yields the slow enhancement rates R_{ge2}. In Fig. 2(b), the fitting Arrhenius plot gives the thermal activation energy of 0.31 ± 0.02 eV, which is a little smaller than the given value of 0.4 ± 0.1 eV in the contribution of Veith et al. [20]. The contradiction may result from the different deposition conditions of Al_2O_3 films or the different thermal treatment processes before illumination.

The subsequently degradation of lifetime in dark is also thermal activated, and Fig. 3(a) shows the effective lifetime of the samples as a function of the time in dark at different temperatures, while Fig. 3(b) plots the degradation rates ln(R_{de}) against the reciprocal of temperatures. The degradation rate is determined by the following double exponential:

$$\tau(t) = A_2 + k_{21}\exp(-R_{de1}t) + k_{22}\exp(-R_{de2}t) \quad (2)$$

where R_{de1}, R_{de2}, A_2, k_{21} and k_{22} are the fast and slow degradation rates and the calculation constants, respectively. It is shown in Fig. 4(a) that the degradation rates of the samples increase with the temperatures, and we can extract the activation energy in the slow degradation process of 0.50 ± 0.07 eV by the fitting Arrhenius plot in Fig. 3(b), which is much large than the activation energy in the enhancement process. It should be noted that the much smaller degradation rate in dark after illumination than the enhancement rate under illumination can be explained by the larger activation energy of the degradation process.

Fig. 4 depicts the C-V curves of the samples during different treatment processes. It is demonstrated in Fig. 4 that the flat band voltage (V_{FB}) of the MIS capacitor moves toward positive voltage direction after

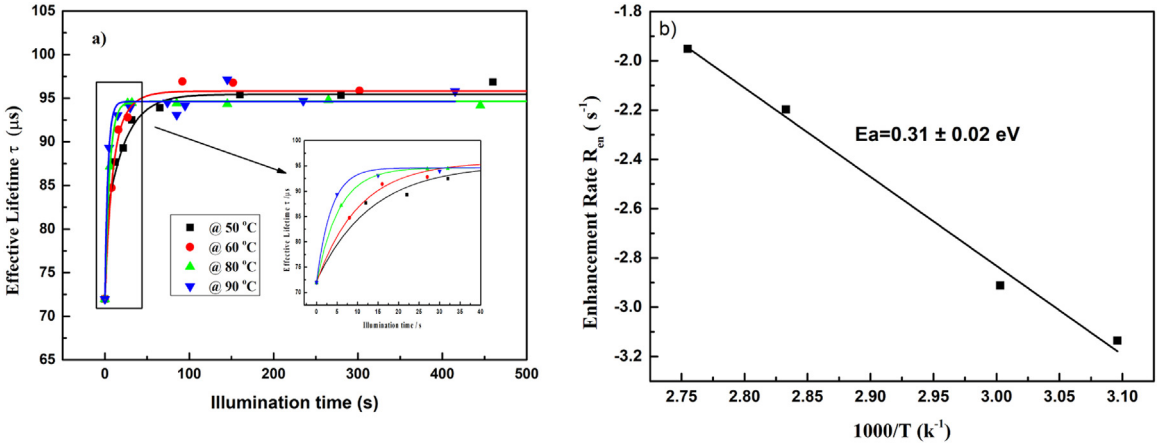

Fig. 2. (a)The effective lifetime dependence of the illumination time with the illumination intensity of 30 mW cm^{-2} at 50 °C, 60 °C, 80 °C and 90 °C, and the inset shows the sharp increase of the effective lifetime in the first 40 s(b)The slow enhancement rates ln(R_{ge2}) as a function of inverse temperature, which yields the activation energy of 0.31 ± 0.02 eV.

1 h's illumination with illumination intensity of 30 mW cm^{-2} at 100 °C. however, the V_{FB} returns to the initial value when the sample was kept in dark at 23 °C for 3 h. Based on these results, we can easily extract the negative charge (Q_f) in the Al_2O_3 dielectric from the following formula:

$$Q_f = \frac{C_o}{q}\left(\varphi_{ms} - V_{FB}\right) \quad (3)$$

where C_o, q, and φ_{ms} are the oxide capacity, elementary charge, and work function differences between Al and *p*-Si, respectively. It can be induced that the negative charge is initially 7.4 × 10^{11} cm^{-2} and gets saturated at the value of 9.1 × 10^{11} cm^{-2} after 1 h's illumination. The increased net negative charge of 1.7 × 10^{11} cm^{-2} can at least partly give rise to the enhancement of the passivation with a sharp increase of the effective lifetime, as the surface recombination velocity has been reported to be inversely proportional to the square of negative charge density near the surface [24].

Fig. 5(a) demonstrates the evolution of increased net negative charge with the illumination time at different temperatures. It can be seen that the net negative charge increases faster at elevated temperatures. We use the double exponential fitting to extract the negative charge increase rate R_{in} by the equation:

$$\Delta Q(t) = A_3 + k_{31}\exp(R_{in1}t) + k_{32}\exp(R_{in2}t) \quad (4)$$

where $\Delta Q(t)$, R_{in1}, R_{in2}, A_3, k_3 are the increased net negative charge at the illumination time *t*, the fast and slow net negative charge increase rates and the calculation constants, respectively. Fig. 5(b) depicts the slow net negative charge increase rate ln(R_{in2}) as a function of the reciprocal of temperatures. The slope of the fitting plot extracts the activation energy of 0.30 ± 0.02 eV for the negative charge increasing process, which is very close to the activation energy value calculated in the lifetime increasing process. These results also give the evidence that the increase of the lifetime under illumination is related to the increase

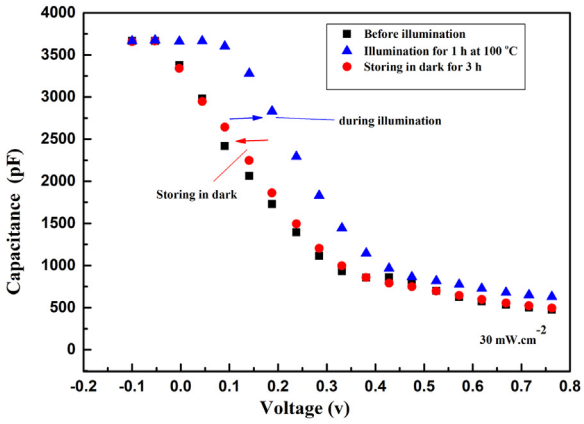

Fig. 4. C-V curves of the samples during different processes: before illumination, after 1 h's illumination with the light intensity of 30 mW cm^{-2} at 100 °C and storing in dark for 3 h at 23 °C after illumination.

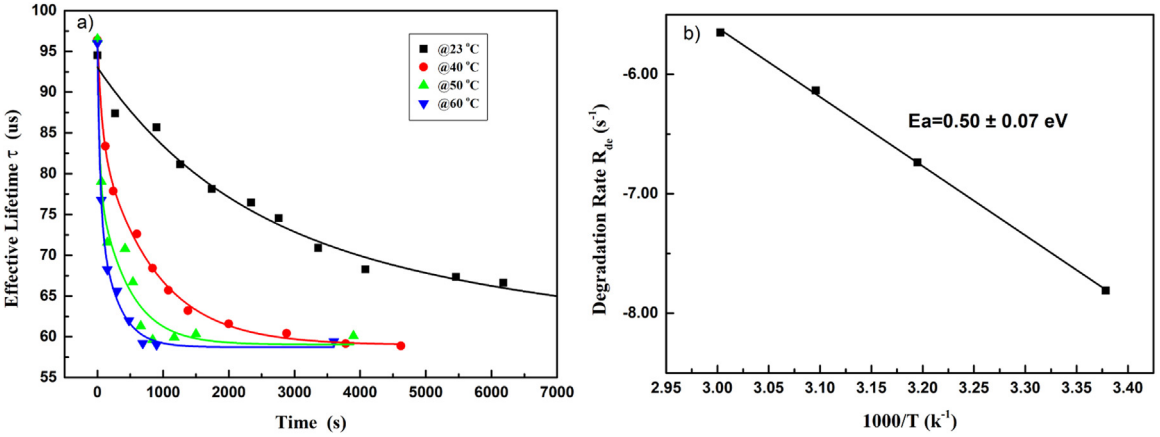

Fig. 3. The plots of effective lifetime as a function of time in dark after illumination at 23–60 °C (a), and the temperature dependence of the degradation rates (b). The slope yields the activation energy of 0.50 ± 0.07 eV.

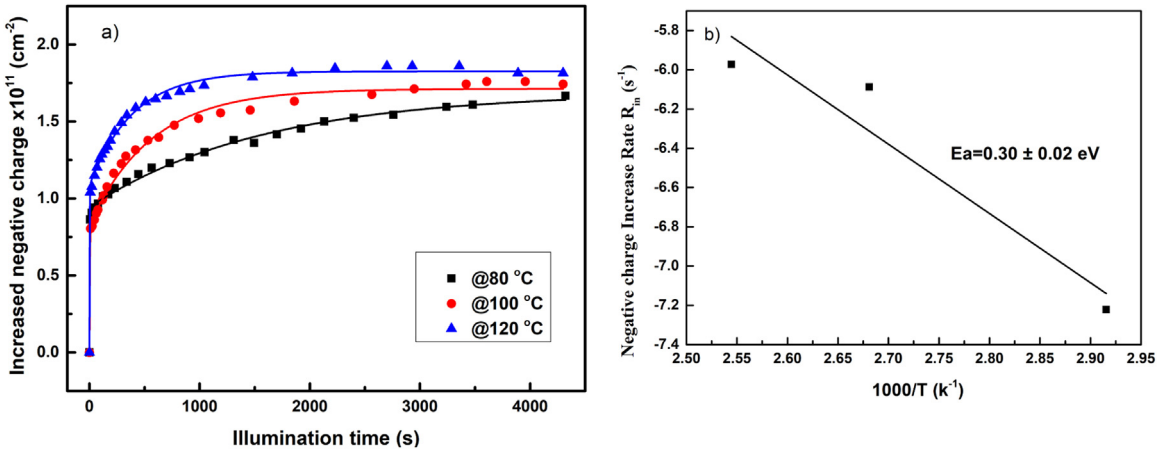

Fig. 5. The evolution of the net negative charge with the illumination time at 80 °C, 100 °C and 120 °C under the illumination intensity of 30 mW cm^{-2} (a) and the Arrhenius plot of the slow negative charge increase rate R_{in2} (b). The slope yields the activated energy of 0.30 ± 0.02 eV.

of negative charge. It should be noted that the negative charge increase rate in Fig. 5 is smaller than that in Fig. 2, which can be attribute to the reduced light intensity by the 50 nm Al electrode for the C-V curve measurement. It has been identified that light intensity has impact on the enhancement rate of the lifetime in the work of Veith et al.[20]

As for the increased negative charge at the surface, it can be owing to the photon-injected electrons trapping which may result from the following models [21,22,25,26]:

I. The injecting photons excite the electrons from the Al_2O_3 valence band to the conduction band, and the excess holes near the Al_2O_3 valence band can react either with the ambient or the silicon substrate, causing the net negative charge [25].
II. The electrons can be excited by the photons from the crystal Si (c-Si) valence band to the conduction band and then tunnel through the ultrathin SiO_x layer directly into Al_2O_3 dielectric and be captured by the trap sites in Al_2O_3 dielectric, leading to the net negative charge [27].
III. The electrons are excited from the c-Si valence band to the Al_2O_3 conduction band by the injecting photons and then the electrons diffuse into the trap sites in the dielectric, giving rise to the increased negative charge in the dielectric [21,22].
IV. The electrons may originate from two-photon processes, where the electrons are firstly excited from the c-Si valence band to the c-Si conduction band and then the electrons in the conduction band of silicon may be excited again to the Al_2O_3 conduction band [28].

In order to have a better understanding of the underlying mechanism of the electron injecting phenomenon, further experiments were conducted with the various LPOFs. Fig. 6(a) shows the effective lifetime as a function of the illumination time for the samples covered by different LPOFs and the reference sample covered with no LPOF under the illumination intensity of 30 mW cm^{-2} at 60 °C. It is demonstrated that the effective lifetime of the samples that are covered by the LPOFs with the cut-off wavelength below 700 nm can increase under illumination, which implies that the photons with the wavelength 700 nm can also induce the electrons trapping. Fig. 6(b) shows the transmittance of the optical filters used in Fig. 6(a). The energy of photons with the wavelength above 700 nm is less than 1.7 eV, which is too small to excite the electron from the Al_2O_3 valence band to the Al_2O_3 conduction band, for the band gap of Al_2O_3 was reported to be 6.8 eV [29,30]. In addition, the c-Si/Al_2O_3 conduction band offset was reported to be 2.02 eV that was not influenced by the ultrathin SiO_x layer in the interface, so the offset between the c-Si valence band and the Al_2O_3 conduction band is about 3.1 eV, taking account of the 1.12 eV band gap of c-Si [21]. So it seems impossible for the photons to excite the electrons from the c-Si valence band to the Al_2O_3 conduction band. For the two-photon process, the 2.02 eV c-Si/Al_2O_3 conduction band offset is also larger than the energy of the photons with the wavelength of 700 nm, which implies that this model seems impossible, either. Based on these results, the model I, model III and model IV mentioned above seem to be contradictory to our experiments. And we propose the electrons trapping and detrapping model (model II) that under illumination the electrons can be excited from the c-Si valence band to the c-Si conduction band and then they can diffuse through the ultrathin SiO_x layer directly into Al_2O_3 dielectric and be captured by the trap sites in Al_2O_3 dielectric, leading to the net negative charge and the enhancement of the passivation. While the trapped electrons can get rid of the trap sites and tunnel back to the *p*-Si substrate and then recombine with the holes if the sample is stored in dark, causing the degradation of the effective lifetime.

Noting that the saturated lifetime under light-soaking for the samples covered by different LPOFs decreases with the cut-off wavelengths. Based on our model, the exited electrons can diffuse through the thin SiO_x layer directly into Al_2O_3 dielectric, where the concentration of excited electron can impact the diffusion. It is obvious that not only the energy but also the intensity of the photons will decrease with the increased cut-off wavelength of the LPOF, so the larger cut-off wavelength will lead to lower concentration of the excited electron in the conduction band of silicon for the samples under the LPOFs, which will also lead to less increased negative charge in the Al_2O_3 dielectric thus lower saturated lifetime of the samples during the light-soaking. In addition, we can see that the lifetime keeps unchanged under illumination when the samples are covered by the LPOFs with the cut-off wavelength of 800 nm and 900 nm. In the work of Lin et al. [31], there is still the passivation enhancement when samples are blocked by the 780 nm LPOF, so we can deduce that the exact cut-off wavelength range causing these light induced enhancement effects is in 780–800 nm. The 1.55 eV energy of the photons with wavelength 800 nm is larger than the 1.12 eV band gap of c-Si, so there should be the light induced enhancement effects for the electrons can be excited from the c-Si valence band to the c-Si conduction band, while in our experiments the lifetime of the sample keeps unchanged. It can be ascribed to the fact that the intensity of photons that transmit though the 800 nm LPOF is too small, and the concentration of excited photon in the c-Si conduction band is very low. Therefore, the trapping and detrapping of electrons actually stand at the equilibrium state, in which case very few electron was trapped in the Al_2O_3 dielectric and no obvious enhancement effect can be observed.

The trapped negative charge density is determined by the trap site density, and the trap site density in the Al_2O_3 dielectric was observed to be influenced by thermal processes [32]. Fig. 7(a) demonstrates the

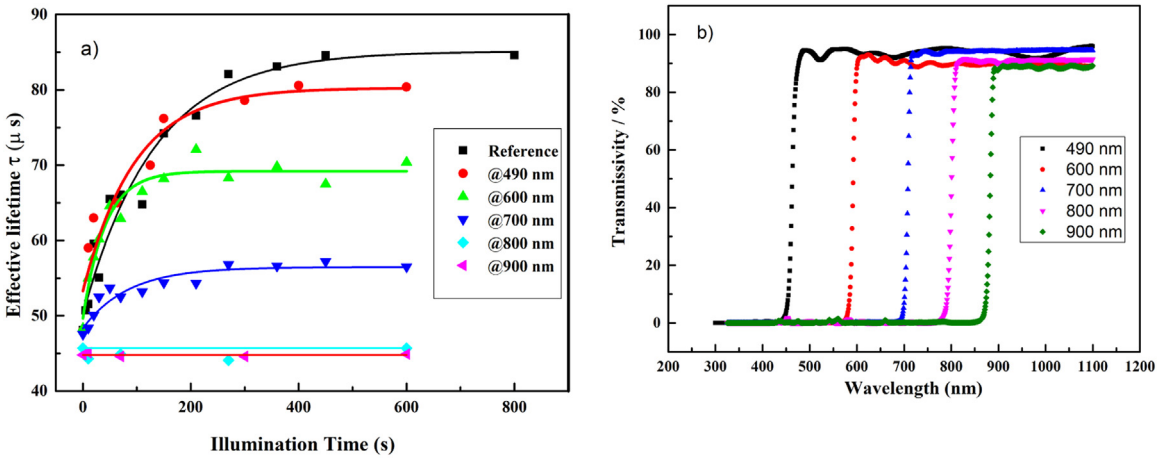

Fig. 6. The plots of the effective lifetime as a function of the illumination time for the samples covered by different LPOFs and the reference sample with no LPOF under illumination of 30 mW cm^{-2} at 60 °C (a). The plots of wavelength versus the transmittance of the optical filters(b). The curves are guided for eyes.

effective lifetime evolution before and after the illumination at 60 °C for the sample that only underwent a 425 °C annealing process and the sample that underwent a 425 °C annealing followed by a 800 °C RTP process. One can see that the effective lifetime increases dramatically from the initial value of 52.8 μs before illumination to the saturated value of 101.8 μs after 1 h's illumination for the sample with 425 °C + 800 °C annealing, and the improvement ratio $\Delta\tau/\tau_0$ is about 0.93, where $\Delta\tau$ is the difference between the saturated effective lifetime value and the initial effective lifetime value, τ_0 is the initial effective lifetime value. However, there is only a slight improvement of the effective lifetime from the initial value of 95.8 μs to the saturated value of 110.4 μs for the sample with only 425 °C annealing. Fig. 7(b) plots the trap site density against the illumination time at 60 °C for different samples. Note that the trap site density D_{tr} is calculated from the flat band shift under illumination by C-V measurements:

$$D_{\mathrm{tr}} = \frac{C_o}{q}\left[V_{FB}(t) - V_{FB}(0)\right] \tag{5}$$

where $V_{FB}(t)$ is the flat band voltage at illumination time t, and $V_{FB}(0)$ is the flat band voltage before illumination. It should be noted that the trap density equals to the increased net negative charge under illumination in our manuscript. As shown in Fig. 7(b), the trap site density for the sample with 425 °C + 800 °C annealing is much larger than that for the sample with only 425 °C annealing, which can explain the obviously different evolution of effective lifetime for the samples in the two groups before and after illumination. Based on these results, we can deduce that the 800 °C RTP process can induce multiple trap sites in the Al_2O_3 dielectric.

4. Conclusions

In summary, we have kinetically investigated the illumination-induced enhancement of the Al_2O_3 passivation on p type silicon. The activation energies of illumination-induced enhancement of the Al_2O_3 passivation and its degradation process are 0.31 ± 0.02 eV and 0.50 ± 0.07 eV, respectively. It was demonstrated that the negative fixed charge at the interface between ultrathin Al_2O_3 film and p-Si substrate increased from 7.4 × 10^{11} cm^{-2} to 9.1 × 10^{11} cm^{-2} after 1 h's illumination and returned to the initial value in dark at room temperature for 3 h. Moreover, it is confirmed that the light induced enhancement effect is wavelength dependent and the cut-off wavelength is in the range of 780–800 nm. Based on these results, we proposed a trapping and detrapping model. The photon-induced electrons in the p-Si substrate could tunnel through the ultrathin SiOx layer and be captured by the traps within the Al_2O_3 layers, and therefore results in the passivation improvement. These results are significant for us to understand the light-soaking enhanced passivation effect of Al_2O_3 on

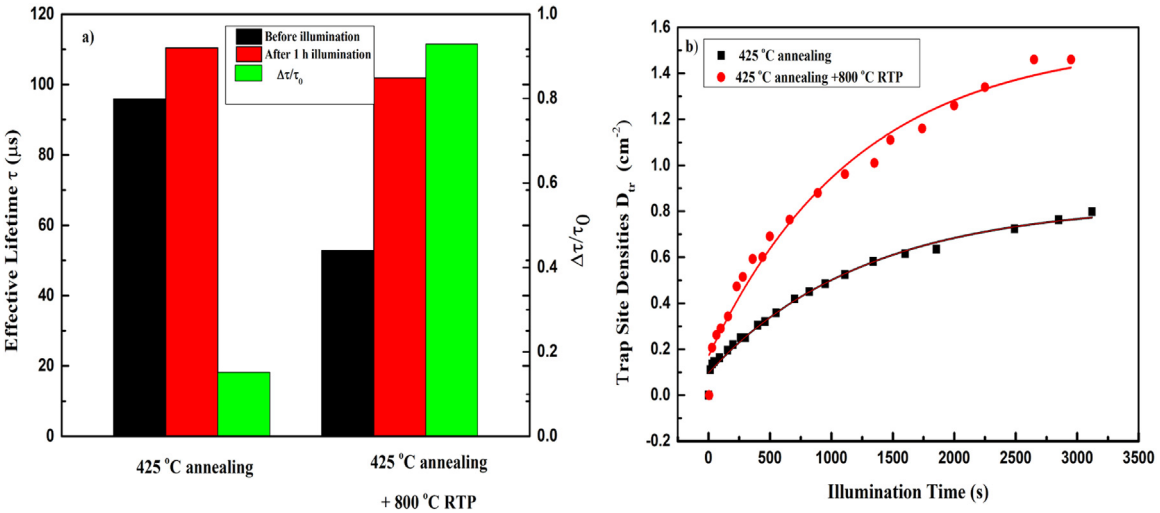

Fig. 7. Effective lifetime changes before and after illumination and the effective lifetime improvement ratio $\Delta\tau/\tau_0$ (a) and the illumination dependence of trap site density at 60 °C for samples that underwent different processes (b).

crystalline silicon surface in photovoltaics.

Acknowledgments

The authors would like to thank National Natural Science Foundation of China (Nos. 51532007, 61574124 and 61721005) and the Science Challenge Project (No. TZ2016003-1) for financial support.

Declarations of interest

none

Appendix A. Supporting information

Supplementary data associated with this article can be found in the online version at doi:10.1016/j.solmat.2018.11.034.

References

[1] B. Veith, T. Dullweber, M. Siebert, C. Kranz, F. Werner, N. Harder, J. Schmidt, B. Roos, T. Dippell, R. Brendel, Comparison of ICP-AlOx and ALD-Al_2O3 layers for the rear surface passivation of c-Si solar cells, Energy Procedia 27 (2012) 379–384.

[2] J. Schmidt, F. Werner, B. Veith, D. Zielke, R. Bock, V. Tiba, P. Poodt, F. Roozeboom, A. Li, A. Cuevas, Industrially relevant Al_2O_3 deposition techniques for the surface passivation of Si solar cells, Open Res. (2010) 1130–1133.

[3] J. Schmidt, A. Merkle, R. Brendel, B. Hoex, M. Van De Sanden, W. Kessels, Surface passivation of high-efficiency silicon solar cells by atomic-layer-deposited Al_2O_3, Prog. Photovolt. Res. Appl. 16 (2008) 461–466.

[4] S. Dauwe, L. Mittelstädt, A. Metz, R. Hezel, Experimental evidence of parasitic shunting in silicon nitride rear surface passivated solar cells, Prog. Photovolt. Res. Appl. 10 (2002) 271–278.

[5] J. Benick, A. Richter, T. Li, N.E. Grant, K.R. Mcintosh, Y. Ren, K.J. Weber, M. Hermle, S.W. Glunz. Effect of a Post-deposition Anneal on Al_2O_3/Si Interface Properties, IEEE, 2010, pp. 891-896.

[6] B. Hoex, J. Schmidt, R. Bock, P.P. Altermatt, M. Van De Sanden, W. Kessels, Excellent passivation of highly doped p-type Si surfaces by the negative-charge-dielectric Al_2O_3, Appl. Phys. Lett. 91 (2007) 112107.

[7] D. Lei, X. Yu, L. Song, X. Gu, G. Li, D. Yang, Modulation of atomic-layer-deposited Al_2O_3 film passivation of silicon surface by rapid thermal processing, Appl. Phys. Lett. 99 (2011) 52103.

[8] B. Hoex, J. Schmidt, P. Pohl, M.C.M. van de Sanden, W.M.M. Kessels, Silicon surface passivation by atomic layer deposited Al_2O_3, J. Appl. Phys. 104 (2008) 44903.

[9] A. Richter, J. Benick, M. Hermle, S.W. Glunz, Excellent silicon surface passivation with 5 Å thin ALD Al_2O_3 layers: Influence of different thermal post-deposition treatments, Phys. Status Solidi (RRL)-Rapid Res. Lett. 5 (2011) 202–204.

[10] G. Dingemans, R. Seguin, P. Engelhart, M. Van De Sanden, W. Kessels, Silicon surface passivation by ultrathin Al2O3 films synthesized by thermal and plasma atomic layer deposition, Phys. Status Solidi (RRL)-Rapid Res. Lett. 4 (2010) 10–12.

[11] K. Kimoto, Y. Matsui, T. Nabatame, T. Yasuda, T. Mizoguchi, I. Tanaka, A. Toriumi, Coordination and interface analysis of atomic-layer-deposition Al_2O_3 on Si (001) using energy-loss near-edge structures, Appl. Phys. Lett. 83 (2003) 4306–4308.

[12] F. Benner, P.M. Jordan, M. Knaut, I. Dirnstorfer, J.W. Bartha, T. Mikolajick. Investigation of the c-Si/Al_2O_3 Interface for Silicon Surface Passivation, 2012.

[13] J. Schmidt, B. Veith, R. Brendel, Effective surface passivation of crystalline silicon using ultrathin Al_2O_3 films and Al_2O_3/SiN_x stacks, Phys. Status Solidi (RRL)-Rapid Res. Lett. 3 (2009) 287–289.

[14] G. Dingemans, P. Engelhart, R. Seguin, F. Einsele, B. Hoex, M. Van de Sanden, W. Kessels, Stability of Al_2O_3 and Al_2O_3/a-SiN_x: H stacks for surface passivation of crystalline silicon, J. Appl. Phys. 106 (2009) 114907.

[15] B. Vermang, H. Goverde, A. Lorenz, A. Uruena, G. Vereecke, J. Meersschaut, E. Cornagliotti, A. Rothschild, J. John, J. Poortmans, R. Mertens. On the blistering of atomic layer deposited Al_2O_3 as Si surface passivation, 2011 in: Proceedings of the 37th IEEE Photovoltaic Specialists Conference, 2011, pp. 3562–3567.

[16] B. Vermang, H. Goverde, A. Uruena, A. Lorenz, E. Cornagliotti, A. Rothschild, J. John, J. Poortmans, R. Mertens, Blistering in ALD Al_2O_3 passivation layers as rear contacting for local Al BSF Si solar cells, Sol. Energ. Mat. Sol. C 101 (2012) 204–209.

[17] L. Hennen, E.H.A. Granneman, W.M.M. Kessels, Analysis of blister formation in spatial ALD Al_2O_3 for silicon surface passivation, 2012 in: Proceedings of the 38th IEEE Photovoltaic Specialists Conference, 2012, pp. 1049–1054.

[18] A. Richter, S. Henneck, J. Benick, M. Hörteis, M. Hermle, S.W. Glunz. Firing stable Al_2O_3/SiN_x layer stack passivation for the front side boron emitter of n-type silicon solar cells, in: Proceedings of the WIP Renewable Energies, Valencia, Spain, 2010, pp. 1453–1456.

[19] T. Lüder, B. Raabe, B. Terheiden. Annealing behavior of Al_2O_3 thin films grown on crystalline silicon by atomic layer deposition, 2010, pp. 2138–2140.

[20] B. Veith, F. Werner, D. Zielke, R. Brendel, J. Schmidt, Comparison of the thermal stability of single Al_2O_3 layers and Al_2O_3/SiN_x stacks for the surface passiviation of silicon, Energy Procedia 8 (2011) 307–312.

[21] J. Gielis, B. Hoex, M. Van de Sanden, W. Kessels, Negative charge and charging dynamics in Al_2O_3 films on Si characterized by second-harmonic generation, J. Appl. Phys. 104 (2008) 73701.

[22] B. Liao, R. Stangl, T. Mueller, F. Lin, C.S. Bhatia, B. Hoex, The effect of light soaking on crystalline silicon surface passivation by atomic layer deposited Al_2O_3, J. Appl. Phys. 113 (2013) 24509.

[23] B. Veith-Wolf, R. Witteck, A. Morlier, H. Schulte-Huxel, M.R. Vogt, J. Schmidt, Spectra-Dependent Stability of the Passivation Quality of Al_2O_3/c-Si Interfaces, IEEE J. Photovolt. 8 (2018) 96–102.

[24] B. Hoex, J. Gielis, M. Van de Sanden, W. Kessels, On the c-Si surface passivation mechanism by the negative-charge-dielectric Al_2O_3, J. Appl. Phys. 104 (2008) 113703.

[25] A.F. Thomson, K.R. Mcintosh, Light-enhanced surface passivation of TiO_2-coated silicon, Prog. Photovolt. Res. Appl. 20 (2012) 343–349.

[26] R. Hezel, K. Jaeger, Low-temperature surface passivation of silicon for solar cells, J. Electrochem. Soc. 136 (1989) 518–523.

[27] S. Kühnhold-Pospischil, P. Saint-Cast, M. Hofmann, S. Weber, P. Jakes, R.A. Eichel, J. Granwehr, A study on Si/Al_2O_3 paramagnetic point defects, J. Appl. Phys. 120 (2016) 195304.

[28] V. Fomenko, E.P. Gusev, E. Borguet, Optical second harmonic generation studies of ultrathin high-k dielectric stacks, J. Appl. Phys. 97 (2005) 83711.

[29] V.V. Afanas, Ev, M. Houssa, A. Stesmans, M.M. Heyns, Band alignments in metal–oxide–silicon structures with atomic-layer deposited Al_2O_3 and ZrO_2, J. Appl. Phys. 91 (2002) 3079–3084.

[30] J. Robertson, Interfaces and defects of high-K oxides on silicon, Solid State Electron. 49 (2005) 283–293.

[31] F. Lin, M.G. Toh, M. Thway, X. Li, N. Nandakumar, X. Gay, B. Dielissen, S. Raj, A.G. Aberle, Impacts of light illumination on monocrystalline silicon surfaces passivated by atomic layer deposited Al_2O_3 capped with plasma-enhanced chemical vapor deposited SiN_x, Jpn. J. Appl. Phys. 56 (2017) 1M–8M.

[32] D. Suh, W.S. Liang, Electrical properties of atomic layer deposited Al_2O_3 with anneal temperature for surface passivation, Thin Solid Films 539 (2013) 309–316.